Inorganica Chimica Acta 375 (2011) 173–180

Contents lists available at ScienceDirect

Inorganica Chimica Acta

journal homepage: www.elsevier.com/locate/ica

Dicopper(II) complexes showing DNA hydrolase activity and monomeric adduct formation with bis(4-nitrophenyl)phosphate

Mithun Roy, Shanta Dhar, Basudev Maity, Akhil R. Chakravarty *

Department of Inorganic and Physical Chemistry, Indian Institute of Science, Sir C.V. Raman Avenue, Bangalore 560012, India

ARTICLE INFO

Article history:
Received 28 January 2011
Received in revised form 25 April 2011
Accepted 30 April 2011
Available online 7 May 2011

Keywords:
Copper
Hydrolytic DNA cleavage
Phenanthroline bases
Crystal structures
Bis(4-nitrophenyl)phosphate adduct
Reaction kinetics

ABSTRACT

Ferromagnetic dicopper(II) complexes $[Cu_2(\mu\text{-}O_2CCH_3)(\mu\text{-}OH)(L)_2(\mu\text{-}L^1)](PF_6)_2$, where L = 1,10-phenanthroline (phen), $L^1 = H_2O$ in **1** and L = dipyrido[3,2-d:2′,3′-f]quinoxaline (dpq), $L^1 = CH_3CN$ in **2**, are prepared and structurally characterized. Crystals of **1** and **2** belong to the monoclinic space group of $P2_1/n$ and $P2_1/m$, respectively. The copper(II) centers display distorted square-pyramidal geometry having a phenanthroline base and two oxygen atoms of the bridging hydroxo and acetate group in the basal plane. The fifth coordination site has weak axially bound bridging solvent molecule H_2O in **1** and CH_3CN in **2**. The Cu···Cu distances are 3.034 and 3.046 Å in **1** and **2**, respectively. The complexes show efficient hydrolytic cleavage of supercoiled pUC19 DNA as evidenced from the mechanistic studies that include T4 DNA ligase experiments. The binuclear complexes form monomeric copper(II) adducts $[Cu(L)_2(BNPP)](PF_6)$ (L = phen, **3**; dpq, **4**) with bis(4-nitrophenyl)phosphate (BNPP) as a model phosphodiester. The crystal structures of **3** and **4** reveal distorted trigonal bipyramidal geometry in which BNPP binds through the oxygen atom of the phosphate. The kinetic data of the DNA cleavage reactions of the binuclear complexes under pseudo- and true-Michaelis–Menten conditions indicate remarkable enhancement in the DNA hydrolysis rate in comparison to the control data.

1. Introduction

Transition metal complexes that are able to cleave DNA under physiological conditions are of importance for various applications in nucleic acids chemistry [1–13]. The double helical structure of DNA could be damaged by two major pathways: (i) hydrolytic cleavage of the phosphodiester linkage or (ii) oxidative DNA cleavage due to sugar and/or nucleobase oxidation. The half-life for hydrolysis of the phosphodiester bond in DNA at neutral pH and 25 °C is estimated to be ~16 million years. The hydrolytic stability of DNA is primarily due to the negatively charged phosphate backbone that inhibits attack by the nucleophiles. DNA hydrolysis could be readily achieved enzymatically. Natural nucleases like purple acid phosphatase, *P*1 nuclease, *S*1 nuclease, endonuclease IV, etc. containing transition metal ions are known to enhance the rate of hydrolysis of DNA to a significant order for cellular function [14–16]. The nucleases which are activated by metal ions are known as metallonucleases. The natural restriction enzymes have been used for cellular applications like recombinant DNA technology. But their large size and limited sequence selectivity prevent their applications for general purpose. It is thus of great interest and importance to develop artificial metallonucleases that show efficient DNA hydrolase activity.

The synthetic metallonucleases catalyzing phosphodiester bond hydrolysis are useful for biochemical and biomedical applications, as DNA conformational probes and chemotherapeutic agents. Earlier reports have shown that lanthanide ions are suitable for hydrolysis of DNA [17–22]. Ruthenium-based complexes are known as efficient synthetic hydrolases [23]. Mononuclear Zn(II)-binding peptide, tethered to a rhodium complex promotes plasmid DNA cleavage with a rate constant of $2.5 \times 10^{-5}\ s^{-1}$ at 37 °C (pH 6.0) [24–26]. Although Fe(III) is present in the active site of some phosphatases, its model complexes are virtually unknown as artificial nucleases. Binuclear diiron(III) complexes of benzimidazolylmethyl derivatives of 1,3-diamino-2-hydroxypropane (HPTB) and 1,4,7-triazaheptane (DTPB) are known to show significant nuclease activity with a rate constant of $\sim 10^{-3}\ s^{-1}$ [27,28]. The cobalt(III) complex of a polyamine ligand cleaves plasmid DNA with a first order rate constant of $5 \times 10^{-5}\ s^{-1}$ [29]. Copper(II) complex of triazacyclononane cleaves DNA at 50 °C (pH 7.8) with a rate constant of $\sim 1.5 \times 10^{-5}\ s^{-1}$ [30,31]. Copper(II) complexes of natural aminoglycosides such as neamine efficiently cleave DNA hydrolytically with a rate constant of $5.2 \times 10^{-4}\ s^{-1}$ [32,33]. We have recently reported $[Cu(dpq)_2(H_2O)](ClO_4)_2$ as a potent model DNA hydrolase showing rate enhancement of 1.55×10^8 fold (dpq, dipyridoquinoxaline) [34].The dppz analog cleaves DNA at a comparatively lower rate than the dpq complex [35].

The present work stems from our continued interest to explore the hydrolytic DNA cleavage potential of copper(II) complexes. We

* Corresponding author. Tel.: +91 80 22932533; fax: +91 80 23600683.
E-mail address: arc@ipc.iisc.ernet.in (A.R. Chakravarty).

0020-1693/$ - see front matter © 2011 Elsevier B.V. All rights reserved.
doi:10.1016/j.ica.2011.04.046

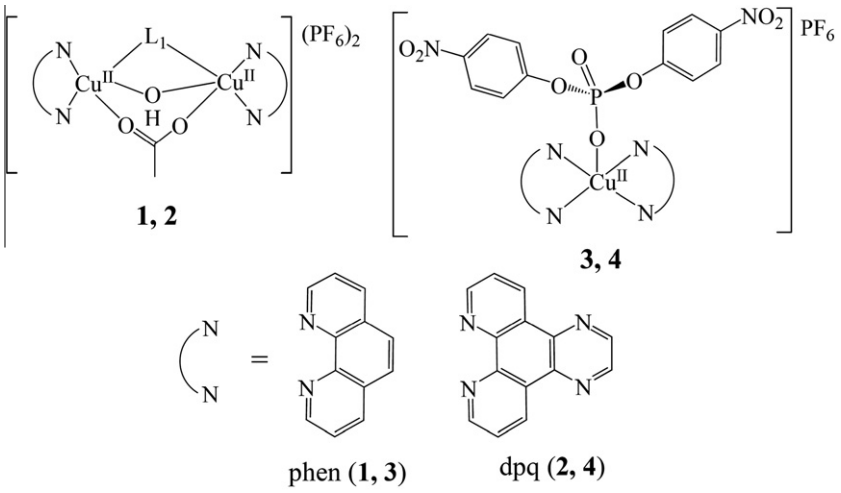

Scheme 1. Dicopper(II) complexes $[Cu_2(\mu\text{-OAc})(\mu\text{-OH})(L)_2(L^1)](PF_6)_2$, where L and L^1 are phen, H_2O in **1** and dpq, CH_3CN in **2**, respectively, and copper(II) complexes $[Cu(L)_2(BNPP)](PF_6)$, where L is phen in **3**, dpq in **4** and BNPP is bis(4-nitrophenyl)phosphate.

have chosen hydroxo and acetato-bridged dicopper(II) complexes considering the presence of labile site(s) in these complexes to significantly promote the rate of hydrolytic DNA cleavage. Herein, we present the synthesis, magnetic properties, crystal structure and hydrolytic DNA cleavage activity of two hydroxo and acetato-bridged dicopper(II) complexes $[Cu_2(\mu\text{-}O_2CCH_3)(\mu\text{-OH})(L)_2(\mu\text{-}L^1)](PF_6)_2$ (**1** and **2**), where L = 1,10-phenanthroline (phen), $L^1 = H_2O$ in **1** and L = dipyrido[3,2-d:2′,3′-f]quinoxaline (dpq), $L^1 = CH_3CN$ in **2** (Scheme 1). Significant result of this study is the remarkable enhancement in the DNA hydrolysis rate in comparison to the control data. We have studied the mechanistic aspects of the DNA cleavage reactions using bis(4-nitrophenyl)phosphate (BNPP) as a model phosphate ester. Structural study on the reaction product show formation of novel monomeric BNPP adduct $[Cu(L)_2(BNPP)](PF_6)$ (L = phen in **3**; dpq in **4**) having copper(II) bound to the phosphate moiety of BNPP (Scheme 1).

2. Experimental

2.1. Materials

All reagents and chemicals were purchased from commercial sources and used without further purification. Calf thymus (CT) DNA, supercoiled (SC) pUC19 DNA (cesium chloride purified), T4 ligase and 5× ligation buffer were purchased from Bangalore Genie (India). Agarose (molecular biology grade), distamycin and ethidium bromide (EB) were from Sigma (USA). Tris(hydroxymethyl)aminomethane–HCl (Tris–HCl) buffer was prepared using deionized and sonicated triple distilled water. Dipyrido[3,2-d:2′,3′-f]quinoxaline (dpq) was prepared following a literature method [36].

2.2. Physical measurements

The elemental analysis was done using a Thermo Finnigan Flash EA 1112 CHNSO analyzer. The infrared and electronic spectra were recorded on Bruker Equinox 55 and Hitachi U-3000 spectrophotometers, respectively. Molar conductivity measurements were done using a Control Dynamics (India) conductivity meter. Variable temperature magnetic susceptibility data in the temperature range 20–300 K were obtained for polycrystalline samples using a George Associates Inc. (Berkeley, USA) Lewis-coil-force magnetometer. $Hg[Co(NCS)_4]$ was used as a standard. Experimental susceptibility data were corrected for diamagnetic contributions [37]. The molar magnetic susceptibilities were fitted by Bleaney–Bowers expression: $\chi_{Cu} = [Ng^2\beta^2/kT][3 + \exp(-2J/kT)]^{-1} + N_\alpha$, where χ is the molar magnetic susceptibility per copper and J is the magnetic exchange parameter, by means of a least-squares program [38].

2.3. Synthesis

2.3.1. Preparation of $[Cu_2(phen)_2(\mu\text{-}O_2CCH_3)(\mu\text{-OH})(\mu\text{-}H_2O)](PF_6)_2$ (*1*) and $[Cu_2(dpq)_2(\mu\text{-}O_2CCH_3)(\mu\text{-OH})(\mu\text{-}CH_3CN)](PF_6)_2$ (*2*)

Complexes **1** and **2** were prepared by a general procedure in which a 0.2 g (0.5 mmol) quantity of dimeric copper(II) acetate.hydrate in 10 ml of aqueous CH_3CN (1:9 v/v) was reacted with the appropriate heterocyclic base (0.9 mmol; phen, 180 mg; dpq, 210 mg) in 15 ml acetonitrile. The solution was stirred for 30 min at 25 °C. The product was obtained as a blue solid in ~85% yield on addition of a solution of $NaPF_6$ (1.0 mmol) in CH_3CN. The solid was isolated, washed with aqueous methanol and dried in vacuum over P_4O_{10}.

Anal. Calc. for $C_{26}H_{22}N_4O_4P_2F_{12}Cu_2$ (**1**): C, 35.83; H, 2.54; N, 6.43. Found: C, 36.02; H, 2.61; N, 6.21%. FT-IR (KBr phase, cm^{-1}): 3355br, 2950w, 2000w, 1830w, 1795w, 1620w, 1580 m, 1425s, 1295s, 1225w, 1150m, 980w, 835vs (PF_6^-), 775m, 670s, 550m, 460w (br, broad; vs very strong; s, strong; m, medium; w, weak). ESI-MS in aqueous CH_3OH: m/z 290.6 $[(M\text{-}2(PF_6)]^{2+}$. UV–Vis in Tris–HCl buffer [λ_{max}, nm (ε, $M^{-1}\,cm^{-1}$)]: 272 (63 280), 293sh (21 290), 708 (80). Λ_M in CH_3CN ($S\,m^2\,M^{-1}$): 255. μ_{eff} at 298 K: 2.06 μ_B/Cu ($2J = 51\ cm^{-1}$).

Anal. Calc. for $C_{32}H_{23}N_9O_3P_2F_{12}Cu_2{\cdot}H_2O$ (**2**·H_2O): C, 37.87; H, 2.48; N, 12.40. Found: C, 37.62; H, 2.61; N, 12.28%. FT-IR (KBr phase, cm^{-1}): 3360br, 3100w, 2360w, 1630w, 1795w, 1560s, 1485m, 1410s, 1210w, 1130m, 1030w, 980w, 830vs (PF_6^-), 730m, 555m, 430w. ESI-MS in H_2O: m/z 354.1 $[(M\text{-}2(PF_6)]^{2+}$. UV–Vis in Tris–HCl buffer [λ_{max}, nm (ε, $M^{-1}\,cm^{-1}$)]: 256 (87 590), 296sh (30 680), 337 (910), 640 (90). Λ_M in CH_3CN ($S\,m^2\,M^{-1}$): 265. μ_{eff} at 298 K: 1.98 μ_B/Cu ($2J = 48\ cm^{-1}$).

2.3.2. Preparation $[Cu(L)_2(BNPP)](PF_6)$ (L = phen, *3*; dpq, *4*)

The precursor complexes were dissolved in water and 1.5 equivalent of bis(4-nitrophenyl)phosphate (BNPP) was added. The reaction mixture was stirred for 4 h at room temperature.

Crystalline complexes were obtained in moderate yield (~30%) by slow evaporation of the solvent.

Anal. Calc. for $C_{36}H_{24}N_6O_8P_2F_6Cu$ (**3**): C, 47.61; H, 2.66; N, 9.25. Found: C, 47.43; H, 2.78; N, 9.02%. FT-IR (KBr phase, cm^{-1}): 3380br, 3078w, 1582m, 1520w, 1430w, 1345m, 1220s, 1160m, 1090m, 835vs (PF_6^-), 640 m, 736s, 624s, 440w. ESI-MS in aqueous DMF: *m*/*z* 761.93 $[(M\text{-}(PF_6)]^+$. UV–Vis in Tris HCl buffer [λ_{max}, nm (ε, $M^{-1}\,cm^{-1}$)]: 272 (115 640), 294 (70 480), 544sh (310), 691br. Λ_M in CH_3CN ($S\,m^2\,M^{-1}$): 140. μ_{eff} (298 K): 1.88 μ_B.

Anal. Calc. for $C_{40}H_{24}N_{10}O_8P_2F_6Cu{\cdot}2H_2O$ (**4**·H_2O): C, 45.83; H, 2.69; N, 13.36. Found: C, 45.62; H, 2.59; N, 13.18%. FT-IR (KBr phase, cm^{-1}): 3360br, 2985w, 2361w, 1585m, 1400w, 1341w, 1225m, 1090m, 895m, 840vs (PF_6^-), 730m, 555m, 435w. UV–Vis in Tris HCl buffer [λ_{max}, nm (ε, $M^{-1}\,cm^{-1}$)]: 297 (78 800), 342 (19 920), 435 (600), 659br. ESI-MS in aqueous DMF: *m*/*z* 866.07 $[(M\text{-}(PF_6)]^+$. Λ_M in CH_3CN ($S\,m^2\,M^{-1}$): 155. μ_{eff} (298 K): 1.91 μ_B.

2.3.3. Solubility and stability

The complexes showed good solubility in water and DMF. The complexes showed stability in the solution phase and this was evidenced from the time dependent UV–Vis spectral measurements. The complexes showed essentially single molecular ion peak in the mass spectra in aqueous DMF suggesting the stability of the complexes in solution.

2.4. X-ray crystallography

2.4.1. Data collection and processing

The green colored block-shaped single crystals of **1** and **2**·H_2O were obtained by diffusion technique in which diethyl ether was layered on the top of the CH_3CN solution of the complexes. Single crystals of **3** and **4**·H_2O were obtained from slow evaporation of the mother liquor in a period of ~2 days. Crystals of respective sizes $0.39 \times 0.31 \times 0.27$, $0.34 \times 0.26 \times 0.23$, $0.37 \times 0.31 \times 0.24$ and $0.38 \times 0.33 \times 0.28\ mm^3$ for **1**–**4** were mounted on glass fibers using epoxy cement and the intensity data were collected using a Bruker SMART APEX CCD diffractometer having a fine focus 1.75 kW sealed tube Mo Kα X-ray source with increasing ω (width of 0.3° $frame^{-1}$) at a scan speed of 15 s per frame. Intensity data were corrected for Lorentz-polarization effects. Empirical absorption corrections were made using the SADABS program [39].

2.4.2. Structure solution and refinement

The structures were solved by heavy-atom method and refined by full matrix least-squares using SHELX system of programs [40]. All non-hydrogen atoms were refined anisotropically. However, the F1, F1A, F4 and F4A atoms of the PF_6^- anion in **3** were refined isotropically due to positional disorder. The hydrogen atoms attached to the carbon atoms were placed at their fixed positions, assigned isotropic thermal parameters and refined using a riding model for structure factor calculation only. The perspective views of the complexes were obtained using ORTEP program [41]. Selected crystallographic data for the complexes are given in Table 1.

2.5. DNA cleavage experiments

The hydrolytic DNA cleavage activity of the complexes **1** and **2** was studied by 0.8% agarose gel electrophoresis in a dark room. Supercoiled pUC19 DNA in Tris–HCl/NaCl buffer (pH 7.2, 50 mM) was treated with varied concentration of the complexes (10–100 μM) in double-distilled water in absence of any external additives. The hydrolytic DNA cleavage reaction was carried out under pseudo Michaelis–Menten condition. Subsequently, the reaction was performed under the true Michaelis–Menten condition with varying the concentration of DNA (30–150 μM) using the complex concentration where maximum rate of the reaction was observed [42]. The samples were incubated for different duration (0–120 min) at 37 °C to determine respective observed rate constants. The concentration of the complexes in water corresponded to the quantity in 2 μL stock solution used prior to dilution to 20 μL final volume using Tris–HCl buffer. After incubation, loading buffer containing 0.25% bromophenol blue, 0.25% xylene cyanol and 30% glycerol (2 μL) was added, and the solution was finally loaded on 0.8% agarose gel containing 1.0 $\mu g\,mL^{-1}$ ethidium bromide (EB). Electrophoresis was carried out in a dark room for 2 h at 45 V in TAE (Tris–acetate–EDTA) buffer. The bands were visualized by UV light and photographed. The extent of cleavage of SC DNA was determined by measuring the intensities of the bands using a UVITECH Gel Documentation System. Due corrections were made for the low

Table 1
Selected crystallographic data for the complexes $[Cu_2(\mu\text{-}OAc)(\mu\text{-}OH)(L)_2(L^1)](PF_6)_2$ (L = phen, $L^1 = H_2O$, **1**; L = dpq, $L^1 = CH_3CN$, **2**) and $[Cu(L)_2(BNPP)](PF_6)$ (L = phen, **3**; dpq, **4**).

	1	**2**·H_2O	**3**	**4**·$2H_2O$
Molecular formula	$C_{26}H_{19}Cu_2F_{12}N_4O_4P_2$	$C_{32}H_{25}Cu_2F_{12}N_8O_4P_2$	$C_{36}H_{24}CuF_6N_6O_8P_2$	$C_{40}H_{28}CuF_6N_{10}O_{10}P_2$
Formula weight ($g\,M^{-1}$)	868.47	1002.62	908.09	1048.20
Crystal system	monoclinic	monoclinic	monoclinic	triclinic
Space group	$P2_1/n$	$P2_1/m$	$P2_1/c$	$P\bar{1}$
a (Å)	8.5089(12)	8.494(4)	12.9613(18)	7.495(4)
b (Å)	18.430(3)	24.676(11)	16.756(2)	11.159(5)
c (Å)	20.530(3)	9.443(4)	17.493(3)	25.048(12)
α (°)	90.00	90.00	90.00	93.261(9)
β (°)	98.312(3)	108.459(8)	107.789(3)	91.323(9)
γ (°)	90.00	90.00	90.00	101.124(9)
V ($Å^3$)	3185.7(8)	1877.3(14)	3617.4(9)	2050.9(17)
Z	4	4	4	2
T (K)	293(2)	293(2)	293(2)	293(2)
ρ_{calc} ($g\,cm^{-3}$)	1.811	1.774	1.667	1.697
λ (Å) (Mo Kα)	0.71073	0.71073	0.71073	0.71073
μ (cm^{-1})	1.547	1.328	0.787	0.713
Data/restraints/parameters	5331 / 0 / 451	3395/0/282	6175/0/530	6829/0/622
F(0 0 0)	1724	1002	1836	1062
Goodness-of-fit (GOF)	1.151	1.211	1.066	1.024
R (F_o)[a], $I > 2\sigma(I)$ [*wR* (F_o)[b]]	0.1156 [0.1970]	0.0932 [0.1973]	0.0968 [0.1932]	0.0974 [0.2102]
R (all data) [*wR* (all data)]	0.1823 [0.2249]	0.1256 [0.2128]	0.1652 [0.2255]	0.1493 [0.2406]

[a] $R = \sum||F_o| - F_c||/\sum F_o$.

[b] $wR = \{\sum[w(F_o^2 - F_c^2)^2]/\sum[w(F_o)^2]\}^{1/2}$; $w = [\sum^2(F_o)^2 + (AP)^2 + BP]^{-1}$, where $P = (F_o^2 + 2F_c^2)/3$, $A = 0.0875$, $B = 4.8244$ for **1**; $A = 0.0931$; $B = 2.2471$ for **2**·H_2O; $A = 0.0966$, $B = 5.6159$ for **3** and $A = 0.1348$, $B = 0.9479$ for **4**·H_2O.

level of nicked circular (NC) form present in the original supercoiled (SC) DNA sample and for the low affinity of EB binding to SC compared to NC and linear forms of DNA [43]. The error range observed in determining %NC form from the gel electrophoresis experiments was ±3–5%.

For the T4 religation experiments, the NC DNA obtained from the hydrolytic cleavage reaction, was recovered from the agarose gel using a gel extraction kit (obtained from Bangalore Genie, India) and this was followed by addition of 5× ligation buffer and T4 DNA ligase (1 μL, 4 units). The solution was incubated for 10 h at 16 °C prior to gel electrophoresis. In the inhibition reactions, the additive like distamycin-A or DMSO was added initially to the SC DNA and incubation was performed for 20 min at 37 °C prior to the addition of the complex.

3. Results and discussion

3.1. Synthesis and general properties

Hydroxo and acetato-bridged dicopper(II) complexes, $[Cu_2(\mu\text{-}OAc)(\mu\text{-}OH)(L)_2(\mu\text{-}L^1)](PF_6)_2$, where L = 1,10-phenanthroline (phen), $L^1 = H_2O$ in **1** and L = [3,2-d:2′,3′-f]quinoxaline (dpq), L^1 = MeCN in **2**, are synthesized and their hydrolytic DNA cleavage activity studied (Scheme 1). The complexes are characterized from analytical, spectral and magnetic data (Table 2). To study the binding aspects of the binuclear complexes to DNA, we have isolated products from the reaction of the complexes **1** and **2** with a model phosphodiester, viz. bis(4-nitrophenyl)phosphate (BNPP). The mononuclear copper(II) complexes $[Cu(L)_2(BNPP)](PF_6)$ (L = phen, **3**; dpq, **4**) are structurally characterized by X-ray crystallography. The IR spectra of the complexes display characteristic PF_6 stretching band near 835 cm^{-1}. The complexes are 1:2 electrolytes. The ESI MS spectra of the complexes display essentially the molecular ion peak suggesting stability of the binuclear structure in a solution phase. The electronic spectra of the complexes are recorded in Tris–HCl buffer medium (pH 7.2). Complexes **1** and **2** display visible band at 708 nm and 640 nm, respectively. The bands are assignable to the d–d transition. The intense electronic bands observed in the UV region are due to π–π* or n–π* electronic transitions.

3.2. X-ray crystallography

Binuclear copper(II) complexes **1** and **2** are crystallized in $P2_1/n$ and $P2_1/m$ space group of the monoclinic crystal system, respectively. The complexes have a (μ-hydroxo)(μ-acetato)(μ-H_2O/MeCN)dicopper(II) core in which each copper(II) center displays distorted square pyramidal geometry with a structural distortion parameter (τ) value of 0.13 and 0.19 for **1** and 0.035 for **2**. Structural distortion parameter is defined as $\tau = (\beta - \alpha)/60$ in a five coordinate structure giving the degree of distortion ranging between trigonal bipyramidal (TBP with τ = 1.0 for 100% TBP) and square pyramidal (SPY with τ = 0.0 for 100% SPY) structure [44]. The perspective views of the complexes are shown in Figs. 1 and 2. The *N*,*N*-donor heterocyclic base, viz. 1,10-phenanthroline (phen) in complex **1** and dipyrido[3,2-d:2′,3′-f]quinoxaline (dpq) in complex **2**, binds at the basal plane. The phenanthroline base is involved in π–π stacking interaction with another base belonging to another molecule. The distances between two copper centers in the complexes **1** and **2** are 3.034 Å and 3.049 Å, respectively, with respective Cu–OH–Cu angle of 103.70(3)° and 104.78(6)°. The axial coordination site of the copper centers is occupied by a solvent water molecule in **1** and CH_3CN in **2**. The axial ligands are showing $\mu\text{–}\eta^2$ binding mode to the metal centers [45–50]. Aqua ligand showing such a binding mode is known for other dicopper(II) complexes [45–48]. The MeCN ligand showing a $\mu\text{–}\eta^2$ binding mode is reported for dimolybdenum and ditungsten complexes [49,50]. The distances of the donor atom of the weakly bound solvent molecule from the copper(II) centers are 2.443(6) Å and 2.413(7) Å in **1** and 2.590(8) Å in **2**. The structural features of complex **1** are similar to those reported for the 2,2'-

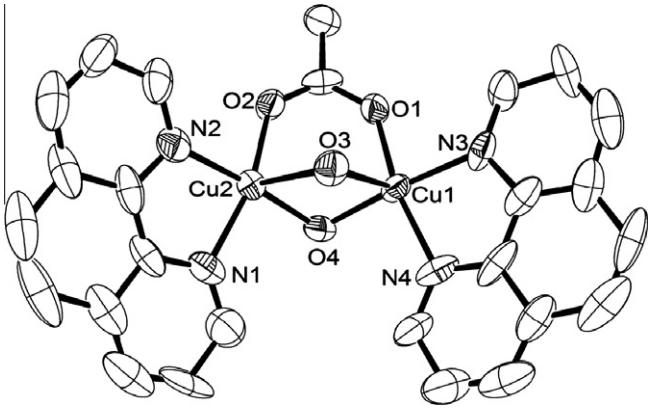

Fig. 1. An ORTEP view of the cationic complex in $[Cu_2(\mu\text{-}O_2CCH_3)(\mu\text{-}OH)(phen)_2(\mu\text{-}H_2O)](PF_6)_2$ (**1**) with 50% probability thermal ellipsoids and the atom numbering scheme for the metal and hetero atoms. Hydrogen atoms are not shown for clarity.

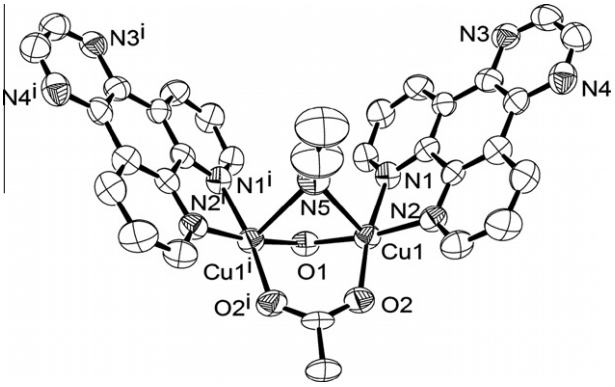

Fig. 2. An ORTEP view of the cationic complex in $[Cu_2(\mu\text{-}O_2CCH_3)(\mu\text{-}OH)(dpq)_2(\mu\text{-}CH_3CN)](PF_6)_2{\cdot}H_2O$ (**2**·H_2O) with 50% probability thermal ellipsoids and the atom numbering scheme for the metal and hetero atoms. Hydrogen atoms are not shown for clarity.

Table 2
Selected physicochemical data for the complexes $[Cu_2(\mu\text{-}OAc)(\mu\text{-}OH)(L)_2(L^1)](PF_6)_2$ (L = phen, $L^1 = H_2O$, **1**; L = dpq, $L^1 = CH_3CN$, **2**) and $[Cu(L)_2(BNPP)](PF_6)$ (L = phen, **3**; dpq, **4**).

Complex	1	2
IR[a] (cm^{-1}) [μ (PF_6^-)]	835	830
ESI-MS[b] (*m*/*z*)	290.6 $[(M-2(PF_6)]^{2+}$	354.1 $[(M-2(PF_6)]^{2+}$
Visible band[c]: λ_{max} (nm) (ε (M^{-1} cm^{-1}))	708 (80)	640 (90)
Λ_M[d] (S m^2 M^{-1})	255	265
μ_{eff}[e] (μ_B)	2.06	1.98
2*J* [f] (cm^{-1})	51	48

[a] KBr phase.
[b] In aqueous MeOH.
[c] In Tris–HCl buffer. The bands are assigned to the copper(II) d–d transition.
[d] Molar conductivity in CH_3CN.
[e] Magnetic moment at 298 K using solid powdered samples of the complexes.
[f] Magnetic exchange parameter.

bipyridine and 1,10-phenanthroline complexes having (μ-hydroxo)(μ-acetato)dicopper(II) core [46,47].

Complexes **3** and **4** crystallize in the monoclinic space group $P2_1/c$ and triclinic space group $P\bar{1}$, respectively. The perspective views of the molecules are shown in Figs. 3 and 4. The complexes are monomeric having each copper(II) center bound to two phenanthroline bases and bis(4-nitrophenyl)phosphate binds to copper via phosphate oxygen atom. The copper centers have an essentially trigonal bipyramidal (TBP) structure with distortion parameter (τ) values of 0.87 and 0.57 for **3** and **4**, respectively (τ = 1.0 for 100% TBP) [44]. It is apparent from the τ value that complex **3** has an essentially TBP geometry. The axial Cu–N distances (1.996(6) Å and 1.979(6) Å) of complex **3** are shorter than the equatorial Cu-N and Cu–O distances (2.043(6) Å, 2.058(5) Å and 2.098(6) Å). The N2–Cu–N4 angle of 178.7(3)° is essentially linear, while the other angles involving the equatorial atoms range within 108.4(2)° to 126.5(2)°. The axial N1–Cu1–N5 angle in **4** is 172.5(2)°. The angles among the equatorial atoms are 96.4(2)°, 124.9(2)° and 138.5(2)°. The angles observed between the axial and equatorial atoms are in the range of 81.7(2)° to 97.9(2)°. The Cu–O distances involving BNPP for the complexes **3** and **4** are 2.043(6) Å and 2.143(5) Å, respectively. The phenanthroline rings in **3** are involved in π–π stacking interactions with another phenanthroline ring of a different molecule. Each of the dpq ring in **4** is involved in π–π stacking interaction with one of BNPP nitrobenzene ring as well as one ring of another molecule. The dihedral angle between the dpq (containing N5–N8 atoms) and the phen ring of BNPP (C35–C40 atoms) is 2.78°, whereas the other dpq ring gives a dihedral angle of 5.93° with another phenyl ring of the BNPP moiety. Two dpq rings of **4** have a dihedral angle of 44.07°. Complex **4**·H_2O shows significant hydrogen-bonding interactions involving the solvent water molecule, one phosphate oxygen atom of BNPP and another solvent water molecule giving distances of 2.742 Å and 2.855 Å. Crystal structures of **3** and **4** suggest conversion of the binuclear core of **1** and **2** to the stable mononuclear phosphate adduct having 1:2 ratio of copper and the phenanthroline base.

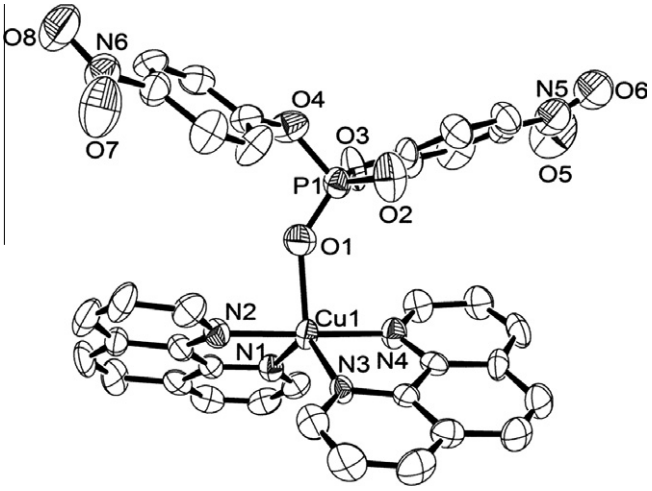

Fig. 3. An ORTEP view of the cationic complex in $[Cu(phen)_2(BNPP)](PF_6)$ (**3**) with 50% probability thermal ellipsoids and the atom labeling scheme for the metal and hetero atoms. Hydrogen atoms are not shown for clarity.

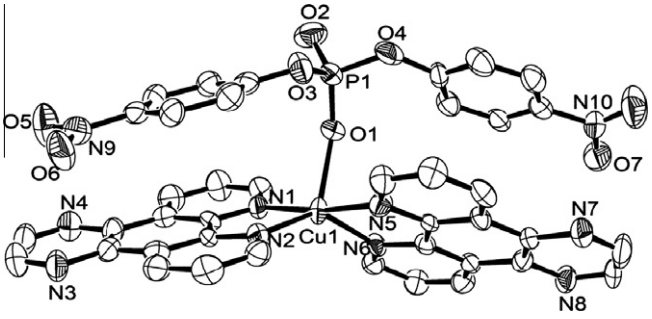

Fig. 4. An ORTEP view of the cationic complex in $[Cu(dpq)_2(BNPP)](PF_6)\cdot H_2O$ (**4**·H_2O) with 50% probability thermal ellipsoids and the atom numbering scheme for the metal and hetero atoms. Hydrogen atoms are omitted for clarity.

3.3. Magneto-structural properties

The variable temperature magnetic susceptibility data of the complexes **1** and **2** show the presence of ferromagnetically coupled dicopper(II) units giving 2J values of 51 and 48 cm^{-1}, respectively, with a g value of 2.0023 (Fig. 5). The magnetic behavior compares well with the 2J values reported for other hydroxo/alkoxo and carboxylato-bridged dicopper(II) complexes [51]. The magneto-structural correlation on complexes having (μ-hydroxo/alkoxo)(μ-acetato)dicopper(II) cores has revealed that the 2J value is dependent on the monoatomic hydroxo/alkoxo bridge angle. Besides, the presence of a 3-atom carboxylato bridge makes the superexchange pathways non-complementary thus reducing the magnitude of 2J [52–54]. A Cu–OH–Cu angle of <110° in the "essentially tribridged" dicopper(II) cores makes the complexes ferromagnetic. The significantly high value of J for the complexes **1** and **2** could be due to the presence of low Cu–OH–Cu angle of ~104°. Christou and coworkers have reported a 2J value of 38.6 cm^{-1} for $[Cu_2(OH)(O_2CMe)(H_2O)(bpy)_2](ClO_4)_2$ [45]. Based on the linear correlation: $-2J = 10.77\phi - 1198$ cm^{-1}, where ϕ is the Cu–OH–Cu angle, we expect 2J value of 78 cm^{-1} for a ϕ angle

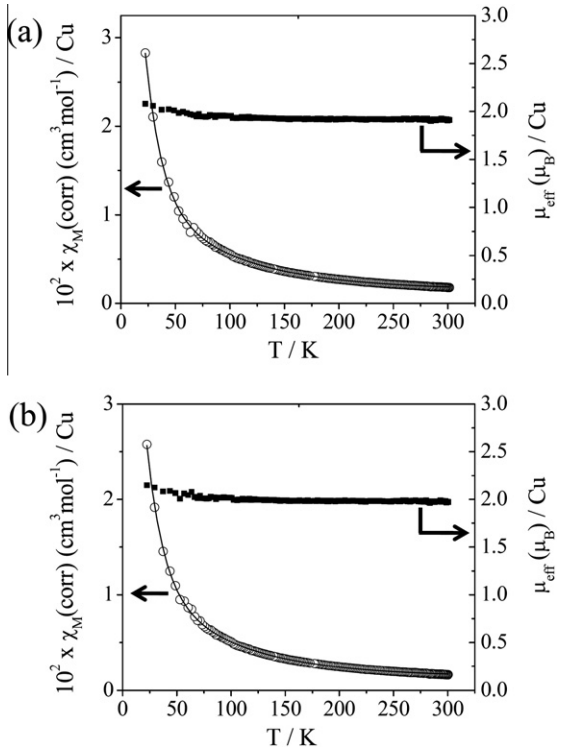

Fig. 5. Plots showing molar magnetic susceptibility per copper (χ_M/Cu) and the effective magnetic moment per copper (μ_{eff}/Cu) versus temperature (T) for the complexes **1** (a) and **2** (b). Theoretical fits of the magnetic data are shown by the solid line in the χ_M/Cu plots.

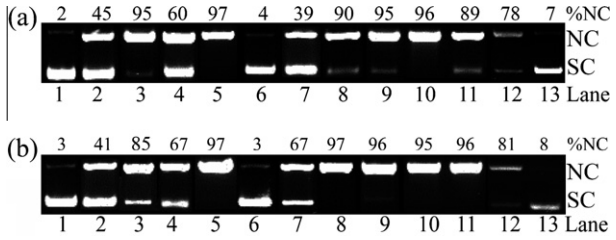

Fig. 6. (a) Agarose gel (0.8%) electrophoresis diagram showing the cleavage of SC pUC19 DNA (60, 120 μM) by complex **1** in dark in Tris buffer (pH 7.2): lane-1, DNA (120 μM) control; lane-2, DNA (120 μM) + **1** (40 μM), 5 min; lane-3, DNA (120 μM) + **1** (40 μM), 30 min; lane-4, DNA (120 μM) + **1** (80 μM), 5 min; lane-5, DNA (120 μM) + **1** (80 μM), 30 min; lane-6, DNA (60 μM) control; lane-7, DNA (60 μM) + **1** (80 μM), 10 min; lane-8, DNA (60 μM) + **1** (80 μM), 60 min; lane-9, DNA (120 μM) + **1** (80 μM), 30 min (in argon); lane-10, DNA (120 μM) + NaN_3 (500 μM) + **1** (80 μM), 30 min; lane-11, DNA (120 μM) + DMSO (4 μL) + **1** (80 μM), 30 min; lane-12, NC form obtained from the treatment DNA (120 μM) + **1** (80 μM) as control without addition of T4 DNA ligase; lane-13, conversion of NC (obtained from DNA (120 μM) + **1** (80 μM)) to SC DNA on treatment with T4 DNA ligase (4 units). (b) Agarose gel (0.8%) electrophoresis diagram showing the cleavage of SC pUC19 DNA by complex **2** in dark in Tris buffer (pH 7.2): lane-1, DNA (120 μM) control; lane-2, DNA (120 μM) + **2** (20 μM), 5 min; lane-3, DNA (120 μM) + **2** (20 μM), 15 min; lane-4, DNA (120 μM) + **2** (60 μM), 5 min; lane-5, DNA (120 μM) + **2** (60 μM), 15 min; lane-6, DNA (60 μM) control; lane-7, DNA (60 μM) + **2** (60 μM), 5 min; lane-8, DNA (60 μM) + **2** (60 μM), 15 min; lane-9, DNA (120 μM) + **2** (60 μM), 15 min (under argon); lane-10, DNA (120 μM) + NaN_3 (500 μM) + **2** (60 μM), 15 min; lane-11, DNA (120 μM) + DMSO (4 μL) + **2** (60 μM), 15 min; lane-12, NC form obtained from the treatment DNA (120 μM) + **2** (60 μM) as control without addition of T4 DNA ligase; lane-13, conversion of NC (obtained from DNA (120 μM) + **2** (80 μM)) to SC DNA on treatment with T4 DNA ligase (4 units).

of 104° [51]. The observed lower 2*J* value from the predicted one could be due to the presence of an axially bound bridging solvent molecule that could enhance the counter-complementary effect of the acetate bridge.

3.4. DNA cleavage activity

The ability of the complexes **1** and **2** to cleave supercoiled plasmid DNA under hydrolytic reaction condition has been assessed by 1% agarose gel electrophoresis. The DNA cleavage reaction has been carried out in both dose and time dependent manner. When pUC19 DNA (4 μg, 120 μM) is incubated with 80 μM of complex **1** for 30 min, a significant cleavage of supercoiled (SC) DNA is observed in comparison to the control reaction (Fig. 6(a)). The dpq complex **2** is more active in cleaving DNA hydrolytically than the phen complex **1** (Fig. 6(b)). Control experiments with copper(II) acetate or the phenanthroline base do not show any DNA cleavage activity under similar experimental conditions suggesting the involvement of the complexes in the DNA cleavage reaction. The complexes cleave DNA in dark under argon medium thus excluding formation of any reactive oxygen species (ROS) [25]. Addition of additives like NaN_3 as singlet oxygen scavenger or DMSO as hydroxyl radical scavenger does not inhibit the DNA cleavage activity indicating non-oxidative nature of the DNA cleavage. Hydrolytic nature of the DNA cleavage is confirmed from the T4 ligase experiments [55]. T4 ligase is an enzyme that specifically religates the fragmented DNA into the supercoiled form. Hydrolytic cleavage of DNA involves hydrolysis of the phosphodiester bond forming

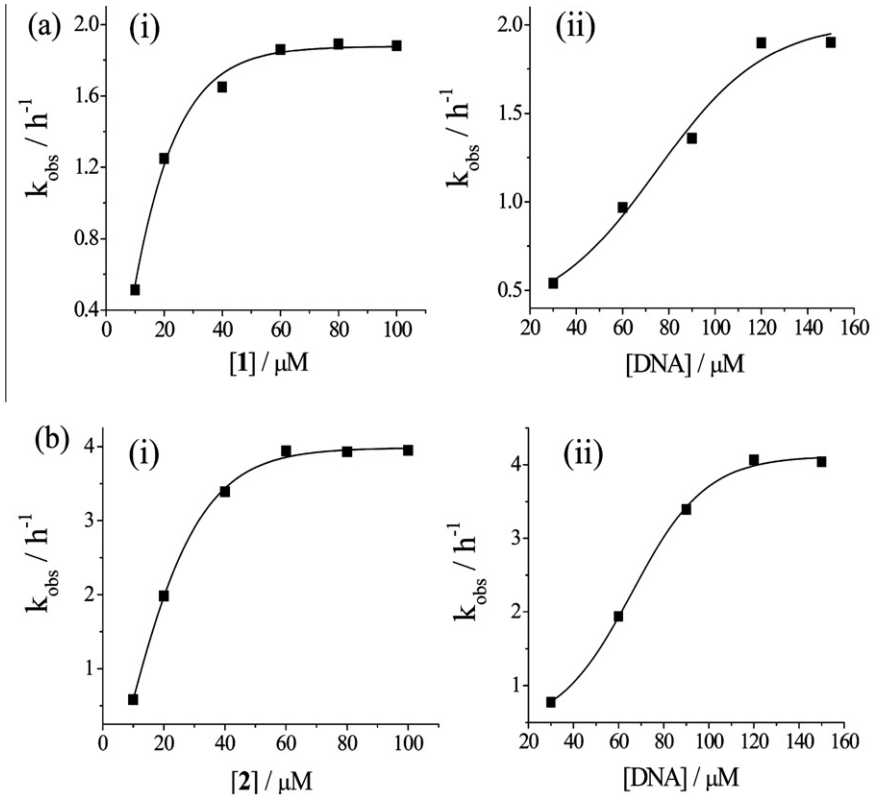

Fig. 7. (a) (i) Plot showing saturation kinetics for the cleavage of pUC19 DNA (120 μM) with different complex concentrations (10–100 μM) of **1** at 37 °C in Tris–HCl buffer (pH 7.2) under pseudo Michaelis–Menten condition and (ii) saturation kinetics of the cleavage of pUC19 DNA using 80 μM complex **1** with different concentrations of the pUC19 DNA (30–150 μM) at 37 °C in Tris–HCl buffer (pH 7.2) under true Michaelis–Menten condition. (b) (i) Plot showing saturation kinetics for the cleavage of pUC19 DNA (120 μM) with different complex concentrations (10–100 μM) of **2** at 37 °C in Tris–HCl buffer (pH 7.2) under pseudo Michaelis–Menten condition and (ii) saturation kinetics of the cleavage of pUC19 DNA using 60 μM complex **2** with different concentrations of the plasmid pUC19 DNA (30–150 μM) at 37 °C in Tris–HCl buffer (pH 7.2) under true Michaelis–Menten condition.

fragments that could be subsequently religated. In contrast, the oxidative cleavage of DNA leads to degradation of the sugar and/or base making the DNA to be permanently damaged and the fragments cannot be religated by T4 ligase. In our T4 ligase experiment, the NC form obtained from the cleavage of SC DNA with the complexes has been reacted with T4 ligase enzyme for overnight and we have observed complete conversion of the NC DNA to its original SC form (Fig. 6).

3.5. Kinetic investigation

The kinetic aspects of the hydrolytic DNA cleavage are studied to obtain the rate of the hydrolytic cleavage. The reactions were done under pseudo-Michaelis–Menten conditions by using various concentrations of **1** (10–100 μM) and constant DNA concentration (120 μM), which results in the formation of nicked circular (NC) DNA from supercoiled (SC) pUC19 DNA [34,35]. The decrease of SC DNA fits well into a single-exponential decay curve and follows pseudo-first-order kinetics as shown in Fig. 7(a, i). The reaction rate constant obtained from the plot is 1.88(± 0.03) h^{-1} with a complex concentration of 80 μM. Under true Michaelis–Menten conditions, in which the complex concentration is kept constant at 80 μM and the DNA concentration is varied from 30–150 μM, we were able to obtain the highest rate constant of 1.90(±0.02) h^{-1} using 120 μM SC DNA (Fig. 7(a, ii)). The Michaelis–Menten constant (K_m) is obtained by means of Lineweaver–Burk method under true Michaelis–Menten conditions [55]. The K_m value and maximum velocity (V_{max}) of the hydrolytic DNA cleavage reaction were calculated to be 1.08×10^{-4} M and 3.03 h^{-1}. Similarly, kinetic aspects of **2** were evaluated under both pseudo and true Michaelis–Menten conditions giving respective rate values of 3.94(±0.03) h^{-1} using 60 μM complex and 4.07(±0.02) h^{-1} at DNA concentration of 120 μM (Fig. 7(b)). The K_m and V_{max} of the hydrolytic DNA cleavage by **2** under true Michaelis–Menten condition from Lineweaver–Burk plot are 8.54×10^{-5} M and 5.95 h^{-1}, respectively. Complexes **1** and **2** show 5.2×10^7 and 1.13×10^8 fold enhancement in the rate of hydrolysis of DNA compared to that of control hydrolysis data.

Table 3
A comparison of the rate values for the hydrolytic cleavage of DNA by selected metal complexes.

Complex	Complex Concentration (μM)	Rate constant (h^{-1})	Rate enhancement[a]	References
(Pr_2^{3+}) ionophore	2000	0.90	2.5×10^7	[56]
Cu (9aneN$_3$)	1000	~0.25	$\sim 1.1 \times 10^6$	[30]
Eu^{3+}	500	0.25	7.0×10^6	[57]
(Eu^{3+}) ionophore	500	2.10	5.83×10^7	[57]
Co^{3+}-cyclen	5000	0.79	2.00×10^7	[58]
Co^{3+}-tamen	1000	0.18	5.00×10^6	[29]
Rh-P-Zn[b]	–	0.09	2.5×10^7	[23]
Ni_2-complex	55	1.27	3.52×10^7	[59]
[Ru(bpy)$_2$BPG]$^{2+}$[c]	20	0.11	3.06×10^6	[60]
Cu-histidine	1000	0.76	–	[61]
Cu-neamine	100	3.57	9.99×10^7	[33]
[Cu(dpq)$_2$(H$_2$O)] (ClO_4)$_2$	55	5.58	1.55x10^8	[34]
[Cu(dppz)$_2$Cl]Cl[d]	55	2.87	7.97×10^7	[35]
1	80	1.90	5.2×10^7	this work
2	60	4.066	1.13×10^8	this work

[a] Rate enhancement compared to the unhydrolyzed ds-DNA rate of 3.6×10^{-8} h^{-1}.
[b] Rh–P, Rh(phi)$_2$bpy-peptide. *In situ* reaction using rhodium complex (5 μM) and $ZnCl_2$ (2.5–20 μM).
[c] BPG = bipyridine-glycoluril.
[d] dppz = Dipyrido-[3,2-*a*:2′,3′-*c*]phenazine.

The observed DNA hydrolysis rate is in good agreement with that of other known metal-based synthetic nucleases (Table 3) [34,56–61]. The higher DNA hydrolase activity of the dpq complex **2** than its phen analog seems to be due to higher DNA binding strength of the dpq ligand with an extended quinoxaline moiety. The observed rate for **2** is less than the mononuclear dpq complex [Cu(dpq)$_2$(H$_2$O)]$^{2+}$ [34]. This could be due to larger steric bulk of **2** inhibiting its binding to DNA phosphate linkage than its monomeric analog [Cu(dpq)$_2$(H$_2$O)]$^{2+}$ or due to greater lability of the axial aqua ligand in the bis-dpq complex than the tri-bridged core in complex **2**.

3.6. Reaction with bis(4-nitrophenyl)phosphate (BNPP)

The Lewis acidity of the metal ions in metallonucleases plays a fundamental role in their catalytic action. The commonly accepted mechanism of DNA hydrolysis involves a nucleophilic attack of water oxygen to phosphorus to give a five-coordinate phosphate intermediate and subsequent rearrangement of the phosphate leading to the DNA cleavage [62]. We have studied the mechanistic aspects of the hydrolytic DNA cleavage using bis(4-nitrophenyl)phosphate (BNPP) as a model phosphodiester. The reaction of BNPP with complexes **1** and **2** leads to the formation of stable monomeric copper(II) BNPP adduct. The complexes isolated are structurally characterized by X-ray crystallography. Since the ESI-MS spectral data suggest solution stability of the binuclear complexes, isolation of monomeric complexes **3** and **4** suggest degradation of the binuclear core on binding to the BNPP molecule and the intermediate species could be a mononuclear bis-phen/dpq complex of copper(II).

4. Conclusions

The hydroxo and acetato-bridged binuclear copper(II) complexes having planar phenanthroline bases are efficient cleavers of plasmid DNA following hydrolytic pathway without involving any external additives or reactive oxygen species. The rate of hydrolysis of DNA has been evaluated under true Michaelis–Menten conditions. The complexes cleave DNA with a rate constant of 1.90 ± 0.02 h^{-1} using 120 μM SC pUC 19 DNA at a complex concentration of 80 μM for **1** with the Michaelis–Menten constant (K_m) of 1.08×10^{-4} M. Similarly, the rate constant for complex **2** is 4.07 ± 0.02 h^{-1} at a complex concentration of 60 μM with K_m value of 8.54×10^{-5} M. We have observed ~10^8-fold rate enhancement in the hydrolytic DNA cleavage reaction compared to that of the control data. Possible intermediate in the hydrolysis of DNA has been explored using bis(4-nitrophenyl)phosphate (BNPP) as a model phosphodiester. The X-ray structures of the products isolated from the reactions of BNPP with the binuclear complexes show formation of monomeric copper(II) complexes of the phenanthroline bases having BNPP bound to copper(II) in trigonal bipyramidal geometry.

Acknowledgements

We thank the Department of Science and Technology (DST), Government of India, for financial support (SR/S5/MBD-02/2007) and the CCD diffractometer facility. A.R.C. thanks DST for J.C. Bose national fellowship.

Appendix A. Supplementary material

CCDC 768666, 768667, 768668 and 768669 contain the supplementary crystallographic data for complexes **1**, **2**, **3** and **4**, respectively. These data can be obtained free of charge from The Cambridge Crystallographic Data Centre via www.ccdc.cam.ac.uk/

data_request/cif. Supplementary data associated with this article can be found, in the online version, at doi:10.1016/j.ica.2011.04.046.

References

[1] N. Hadjiliadis, E. Sletten, Metal Complex–DNA Interactions, John Wiley and Sons Ltd., Chichester, 2009.
[2] D.S. Sigman, A. Mazumder, D.M. Perrin, Chem. Rev. 93 (1993) 2295.
[3] G. Pratviel, J. Bernadou, B. Meunier, Angew. Chem., Int. Ed. 34 (1995) 746.
[4] C. Metcalfe, J.A. Thomas, Chem. Soc. Rev. 32 (2003) 215.
[5] B.M. Zeglis, V.C. Pierre, J.K. Barton, Chem. Commun. (2007) 4565.
[6] K.E. Erkkila, D.T. Odom, J.K. Barton, Chem. Rev. 99 (1999) 2777.
[7] H.T. Chifotides, K.R. Dunbar, Acc. Chem. Res. 38 (2005) 146.
[8] W.K. Pogozelski, T.D. Tullius, Chem. Rev. 98 (1998) 1089.
[9] C.J. Burrows, J.G. Muller, Chem. Rev. 98 (1998) 1109.
[10] L.K.J. Boerner, J.M. Zaleski, Curr. Opin. Chem. Biol. 9 (2005) 135.
[11] E.L. Hegg, J.N. Burstyn, Coord. Chem. Rev. 173 (1998) 133.
[12] S.E. Wolkenberg, D.L. Boger, Chem. Rev. 102 (2002) 2477.
[13] A. Sreedhara, J.A. Cowan, J. Biol. Inorg. Chem. 6 (2001) 337.
[14] C. Liu, L. Wang, Dalton Trans. (2009) 227.
[15] D.J. Hosfield, Y. Guan, B.J. Haas, R.P. Cunningham, J.A. Tainer, Cell 98 (1999) 397.
[16] N. Horton, J.J. Perona, Proc. Natl. Acad. Sci. USA 97 (2000) 5729.
[17] B.K. Takasaki, J. Chin, J. Am. Chem. Soc. 116 (1994) 12.
[18] M. Komiyama, T. Shiiba, T. Kodama, N. Takeda, J. Sumaoka, M. Yashiro, Chem. Lett. 23 (1994) 1025.
[19] A. Roigk, R. Hettich, H.-J. Schneider, Inorg. Chem. 37 (1998) 751.
[20] M.E. Branum, L. Que Jr., J. Biol. Inorg. Chem. 4 (1999) 593.
[21] J. Sumaoka, Y. Azuma, M. Komiyama, Chem. Eur. J. 4 (1998) 205.
[22] J. Sumaoka, T. Igawa, K. Furuki, M. Komiyama, Chem. Lett. 29 (2000) 56.
[23] L.A. Basile, A.L. Raphael, J.K. Barton, J. Am. Chem. Soc. 109 (1987) 7550.
[24] M.P. Fitzsimons, J.K. Barton, J. Am. Chem. Soc. 119 (1997) 3379.
[25] K.D. Copeland, M.P. Fitzsimons, R.P. Houser, J.K. Barton, Biochemistry 41 (2002) 343.
[26] R.H. Terbrueggen, J.K. Barton, Biochemistry 34 (1995) 8227.
[27] L.H. Schnaith, R.S. Hanson, L. Que Jr., Proc. Natl. Acad. Sci. USA 91 (1994) 569.
[28] C. Liu, S. Yu, D. Li, Z. Liao, X. Sun, H. Xu, Inorg. Chem. 41 (2002) 913.
[29] N.E. Dixon, R.J. Geue, J.N. Lambert, S. Moghaddas, D.A. Pearce, A.L. Sargeson, Chem. Commun. (1996) 1287.
[30] E.L. Hegg, J.N. Burstyn, Inorg. Chem. 35 (1996) 7474.
[31] K.M. Deck, T.A. Tseng, J.N. Burstyn, Inorg. Chem. 41 (2002) 669.
[32] A. Sreedhara, J.A. Cowan, Chem. Commun. (1998) 1737.
[33] A. Sreedhara, J.D. Freed, J.A. Cowan, J. Am. Chem. Soc. 122 (2000) 8814.
[34] S. Dhar, P.A.N. Reddy, A.R. Chakravarty, Dalton Trans. (2004) 697.
[35] T. Gupta, S. Dhar, M. Nethaji, A.R. Chakravarty, Dalton Trans. (2004) 1896.
[36] J.G. Collins, A.D. Sleeman, J.R. Aldrich-Wright, I. Greguric, T.W. Hambley, Inorg. Chem. 37 (1998) 3133.
[37] R.L. Dutta, A. Syamal, Elements of Magnetochemistry, Affiliated East–West Press, New Delhi, 1993.
[38] C.J. O'Connor, Prog. Inorg. Chem. 29 (1982) 203.
[39] G.M. Sheldrick, SADABS, Version 2. Multi-Scan Absorption Correction Program, Universität Göttingen, Göttingen, Germany, 2001.
[40] G.M. Sheldrick, SHELX-97, Programs for Crystal Structure Solution and Refinement, Universität Göttingen, Göttingen, Germany, 1997.
[41] C.K. Johnson, ORTEP, III Report ORNL – 5138, Oak Ridge National Laboratory, Oak Ridge, TN.
[42] A.G. Marangoni, Enzyme Kinetics: A Modern Approach, John Wiley and Sons Inc., Hoboken, New Jersey, 2003.
[43] J. Bernadou, G. Pratviel, F. Bennis, M. Girardet, B. Meunier, Biochemistry 28 (1989) 7268.
[44] A.W. Addison, T.N. Rao, J. Reedijk, G.C. Verschoor, J. Chem. Soc., Dalton Trans. (1984) 1349.
[45] G. Christou, S.P. Perlepes, E. Libby, K. Folting, J.C. Huffman, R.J. Webb, D.N. Hendrickson, Inorg. Chem. 29 (1990) 3657.
[46] T. Tokii, N. Hamamura, M. Nakashima, Y. Muto, Bull. Chem. Soc. Jpn. 65 (1992) 1214.
[47] P. Baran, R. Boca, M. Breza, H. Elias, H. Fuess, V. Jorik, R. Klement, I. Svoboda, Polyhedron 21 (2002) 1561.
[48] P. Talukder, S. Sen, S. Mitra, L. Dahlenberg, C. Desplanches, J.-P. Sutter, Eur. J. Inorg. Chem. (2006) 329.
[49] F.A. Cotton, L.M. Daniels, C.A. Murillo, X. Wang, Polyhedron 17 (1998) 2781.
[50] J.L. Elgin, E.M. Hines, E.J. Valente, J.D. Jubkowski, Inorg. Chim. Acta 229 (1995) 113.
[51] K. Geetha, M. Nethaji, N.Y. Vasanthacharya, A.R. Chakravarty, J. Coord. Chem. 47 (1999) 77.
[52] C. López, R. Costa, F. Illas, C. de Graaf, M.M. Turnbull, C.P. Landee, E. Espinosa, I. Matae, E. Molinse, Dalton Trans. (2005) 2322.
[53] L.K. Thompson, S.K. Mandal, S.S. Tandon, J.N. Bridson, M.K. Park, Inorg. Chem. 35 (1996) 3117.
[54] H. Grove, J. Sletten, M. Julve, F. Lloret, J. Chem. Soc., Dalton Trans. (2000) 515.
[55] J. Sambrook, E.F. Fritsch, T. Maniatis, Molecular Cloning: A Laboratory Manual, second ed., 1.53–1.73, 1989.
[56] K.G. Ragunathan, H.J. Schneider, Angew. Chem., Int. Ed. 35 (1996) 1219.
[57] J. Rammo, R. Hettich, A. Roigk, H.J. Schneider, Chem. Commun. (1996) 105.
[58] R. Hettich, H.J. Schneider, J. Am. Chem. Soc. 119 (1997) 5638.
[59] S. Anbu, M. Kandaswamy, B. Varghese, Dalton Trans. 39 (2010) 3823.
[60] M.S. Deshpande, A.A. Kumbhar, A.S. Kumbhar, Inorg. Chem. 46 (2007) 5450.
[61] R. Ren, P. Yang, W. Zheng, Z. Hua, Inorg. Chem. 39 (2000) 5454.
[62] F. Mancin, P. Scrimin, P. Tecillab, U. Tonellato, Chem. Commun. (2005) 2540.